High order numerical methods for solitons in non-linear PDEs

Ross Linscott

February 11, 2014

Abstract

The application of two finite difference schemes is investigated. Korteweg-de Vries' equation and Boussinesq's equation, which are soliton generating non-linear partial differential equations, are used as test problems. A periodic scheme is applied to both Korteweg-de Vries' and Boussinesq's equation, while a summation by parts scheme is applied only to Korteweg-de Vries' equation. Stability is proven and order of accuracy is validated. The summation by parts scheme is applied to a well-posed initial and boundary value problem, while the periodic scheme is applied to a periodic problem. The periodic scheme proves to be of expected order of accuracy, while the summation by parts scheme exhibits good convergence, even exceeding expectations.

Outline

- In Section 2, the continous models are analysed to show stability and obtain a well-posed initial boundary value problem.
- In Section 3, a periodic finite difference discretisation is introduced for the periodic problem. Energy estimates are derived for the schemes, proving stability.
- In Section 3.2, the SBP-SAT spatial discretisation is introduced for the initial and boundary value problem for the Korteweg-de Vries equation.
- In Section 4, we present convergence results for the fully discrete implementations of each model. In addition, the stability region of the Boussinesq model with respect to wave number of colliding waves is investigated.

Contents

1 Introduction and Background **4**

2 The continous models **4**
2.1 Korteweg-de Vries equation 5
2.2 Boussinesq equation 6

3 The Semi-discrete Models **7**
3.1 Periodic case 7
3.1.1 Korteweg-de Vries equation 8
3.1.2 Boussinesq equation 9
3.2 Boundary value problem 10

4 Computations **12**
4.1 Periodic case 12
4.1.1 Korteweg-de Vries equation 12
4.1.2 Boussinesq equation 13
4.2 Boundary value problem 17
4.2.1 Estimating accuracy 17
4.2.2 Estimating CFL condition 18
4.2.3 Test problem 19
4.2.4 Standing waves 19

5 Conclusions and discussion **23**

A Proof that D_3 is an SBP operator **25**

1 Introduction and Background

Solitons are waves that travel whithout loosing their shape or energy. They arise for example in quantum mechanical systems or shallow water systems, and can be modelled by non-linear PDEs.

Finding stable numerical solutions to initial boundary value problems for these equations can be quite difficult; the dispersive wave properties of the problem require a high degree of resolution to avoid large errors. Especially if the problem leads to a stiff ODE, this means a very large number of computations (as the number of required time steps grows in proportion to some power of the number of grid points). Thus, increasing the order of accuracy, and thereby decreasing the required number of grid points, is essential in order to get feasible computation times.

An additional difficulty is handling the boundary conditions in a manner that guarantees stability. Working with provably stable methods is advantageous, because it guarantees convergence.

The summation-by-parts simultaneous approximation term (SBP-SAT) method was developed to meet these needs. It gives stability per construction; the numerical boundary treatment can be adjusted in such a manner that it guarantees stability. At the same time, the scheme has the high order of accuracy required to sufficiently resolve dispersive wave equations. This means that a sufficiently course grid can be used, so that the stiffness does not lead to infeasibly long computation times.

In this study, both Korteweg-de Vries' and Boussinesq's continous models are shown to be stable, though a local linearisation is required in the Boussinesq case. The periodic finite difference scheme is shown to be stable when applied to the periodic formulation of both equations. Order of accuracy is measured and found to match expectations. The SBP-SAT scheme is applied to an initial and boundary value formulation of Korteweg-de Vries' equation, which is also shown to be stable. The measured order of accuracy for this scheme is found to exceed expectations.

2 The continous models

This report addresses the numerical handling of two non-linear PDE models for shallow water waves: the Korteweg-de Vries equation (1) and the Boussinesq equation (2).

$$u_t = -6uu_x - u_{xxx} \tag{1}$$

$$u_{tt} = u_{xx} - 3(u^2)_{xx} - \alpha u_{xxxx} \tag{2}$$

2.1 Korteweg-de Vries equation

Lemma 1. *There exist boundary conditions for which Korteweg-de Vries equation (1) is well-posed.*

Proof. For Korteweg's equation, it is possible to obtain an energy estimate without linearising by noting that $6uu_x = 2uu_x + 2(u^2)_x$. Hence, (1) is rewritten as

$$u_t = -2uu_x - 2(u^2)_x - u_{xxx}.$$

Let us introduce the inner product

$$(a, b) = \int_l^r a(x)b(x)dx,$$

and the energy of the system

$$E = \|u\|^2. \tag{3}$$

Now, multiplying by u, adding the transpose and integrating by parts on some interval $x \in [l, r]$ leads to

$$\begin{aligned}
(u, u_t) + (u_t, u) &= -4(u, uu_x) - 4(u, (u^2)_x) - 2(u, u_{xxx}) \\
&= -4(u, uu_x) - 4\left[u^3\right]_l^r + 4(u_x, u^2) - 2\left[uu_{xx}\right]_l^r + 2(u_x, u_{xx}) \\
&= (-4 + 4)(u, uu_x) + 2\left[\frac{1}{2}u_x^2 - 4u^3 - 2uu_{xx}\right]_l^r \\
&= \left[u_x^2 - 4u^3 - 2uu_{xx}\right]_l^r = BT, \text{ so} \\
(u, u_t) + (u_t, u) &= \frac{d}{dt}\|u\|^2 = E_t = BT.
\end{aligned}$$

For periodic boundaries, $BT = 0$ which gives $E_t = 0$. It is also possible to find boundary conditions which fullfill the energy condition $BT \leq 0$. For example one could set $u = 0$ on both boundaries and $u_x = 0$ on the right boundary. For the problem to be well-posed, we require three boundary conditions, as the principal term is a third order derivative (see [2]). Due to

the u^3 term, we must at least have $u = 0$ at both boundaries. With these two conditions, we see that at least one more condition on u_x is required on the right boundary in order to fullfill the energy condition. This concludes the proof.

□

Let us pose (1) as the initial and boundary value problem (4)

$$\begin{cases} u_t &= -6uu_x - u_{xxx},\ x \in [l, r],\ t \geq 0 \\ u &= g_1(t),\ x = l \\ u &= g_2(t),\ x = r \\ u_x &= h_1(t),\ x = r \\ u &= f(x),\ t = 0 \end{cases} \tag{4}$$

2.2 Boussinesq equation

Lemma 2. *There exist boundary conditions such that the Boussinesq equation (2) has a local linearisation (5) which is well-posed, as long as the linearisation coefficient u_0 fullfills $u_0 \leq \frac{1}{3}$.*

Proof. For the Boussinesq equation (2), the non-linear term is linearised in order to perform an approximate energy analysis. Making the approximation $u^2 \approx u_0 u$, for some constant u_0, we can rewrite (2) as

$$u_{tt} = (1 - 3u_0)u_{xx} - \alpha u_{xxxx}. \tag{5}$$

Now that we have a linear equation, we can use Fourier analysis to show well-posedness. Inserting the Fourier ansats $u = \hat{u}_\omega(t)exp(\imath\omega x)$ into (5) leads to

$$\begin{aligned} \hat{u}_{tt} &= (1 - 3u_0)(-\omega^2)\hat{u} - \alpha(\omega^4)\hat{u} \\ &= -\omega^2(1 - 3u_0 + \alpha\omega^2)\hat{u} \\ &= \lambda\hat{u}. \end{aligned}$$

As long as λ is real and negative, $\hat{u}$ will not grow, which is equivalent to that u will not grow. For this to be true independently of ω, we end up with the requirement $u_0 < \frac{1}{3}$. That is, the linear well-posedness conclusion only holds for sufficiently small solutions.

In order to find well-posed boundary conditions, we employ the energy method and use the fact that we need four boundary conditions (as the principal term is fourth order). Multiplying (5) by u_t, adding the transpose and integrating on $[l, r]$ gives

$$
\begin{aligned}
(u_t, u_{tt}) + (u_{tt}, u_t) &= 2(1-3u_0)(u_t, u_{xx}) - 2\alpha(u_t, u_{xxxx}) \\
&= 2(1-3u_0)\left[u_t u_x\right]_l^r - 2(1-3u_0)(u_{xt}, u_x) \\
&\quad - 2\alpha\left[u_t, u_{xxx}\right]_l^r + 2\alpha(u_{xt}, u_{xxx}) \\
&= -(1-3u_0)\|u_x\|_t^2 - \alpha\|u_{xx}\|_t^2 + BT, \text{ where} \\
BT &= 2\left[(1-3u_0)u_t u_x - \alpha u_t u_{xxx} + \alpha u_{xt} u_{xx}\right]_l^r, \text{ so} \\
\frac{d}{dt}\|u_t\|^2 &= -(1-3u_0)\|u_x\|_t^2 - \alpha\|u_{xx}\|_t^2 + BT
\end{aligned}
$$

Defining the energy of the system as

$$
E = \|u_t\|^2 + (1-3u_0)\|u_x\|^2 + \alpha\|u_{xx}\|^2, \tag{6}
$$

we see that $\frac{dE}{dt} = BT$. As long as $BT \leq 0$, the linearised model is well-posed, so let us call this the energy condition. A possible set of four boundary conditions fullfilling the energy condition is $u = const$ and $u_x = const$ on both boundaries, which gives $BT = 0$. We pose this as an initial and boundary value problem in (7), and consider the proof complete.

□

$$
\begin{cases}
u_{tt} &= u_{xx} - 3(u^2)_{xx} - \alpha u_{xxxx}, x \ \in [l, r], \ t \geq 0 \\
u &= c_1, \ x = l \\
u &= c_2, \ x = r \\
u_x &= c_3, \ x = l \\
u_x &= c_4, \ x = r \\
u &= f_1(x), \ t = 0 \\
u_t &= f_2(x), \ t = 0
\end{cases} \tag{7}
$$

3 The Semi-discrete Models

3.1 Periodic case

In the case of periodic boundary conditions, both equations (1) and (2) can be spatially discretised using periodic finite difference schemes. Let us introduce the periodic derivation matrices $\tilde{D}_1$ and $\tilde{D}_2$. They can be of varying order of accuracy but will fullfill $\tilde{D}_1 = -\tilde{D}_1^{\ T}$, $\tilde{D}_2 = \tilde{D}_2^{\ T} \leq 0$ and $\tilde{D}_1\tilde{D}_2 = \tilde{D}_2\tilde{D}_1$. These matrix operators are applied to a vector v approximating the solution u, taken in the m evenly distributed points $x_j = jh$ ($j \in \{0, .., m-1\}$) over the interval $[-L/2, L/2]$, where $h = \frac{L}{m}$. This means v_j approximates $u(x_j)$.

Note that the left boundary point is included, while the right boundary point is not; as the problem is periodic, these points represent the same point and should not be included twice.

3.1.1 Korteweg-de Vries equation

For equation (1), we can approximate u as v, where

$$v_t = -2\bar{v}\tilde{D}_1 v - 2\tilde{D}_1\bar{v}v - \tilde{D}_1\tilde{D}_2 v, \tag{8}$$

and $\bar{v}$ denotes a diagonal matrix containing the elements of v on its diagonal.

Lemma 3. *The spatially discretised version of (1) given by the ODE (8) is well-posed.*

Proof. An energy estimate can be found by multiplying by v^T from the left, and adding the conjugate transpose. This yields

$$\begin{aligned} v^T v_t + v_t^T v &= -2v^T\bar{v}^T\tilde{D}_1 v - 2v^T{\tilde{D}_1}^T\bar{v}^T v - 2v^T\tilde{D}_1\bar{v}^T v - 2v^T\bar{v}^T{\tilde{D}_1}^T v \\ &\quad - v^T\tilde{D}_1\tilde{D}_2 v - v^T{\tilde{D}_2}^T{\tilde{D}_1}^T v \\ &= -2v^T\bar{v}\tilde{D}_1 v + 2v^T\tilde{D}_1\bar{v}v - 2v^T\tilde{D}_1\bar{v}v + 2v^T\bar{v}\tilde{D}_1 v \\ &\quad - v^T\tilde{D}_1\tilde{D}_2 v + v^T\tilde{D}_2\tilde{D}_1 v \\ &= 0, \text{ which gives} \\ \frac{d}{dt}\|v\|_h^2 &= 0, \end{aligned}$$

where we have introduced the h-norm $\|v\|_h^2 = hv^T v$. Using the energy (mimicking the continous energy (3))

$$E = \|v\|_h^2, \tag{9}$$

we get

$$E_t = 0$$

which implies well-posedness.

□

3.1.2 Boussinesq equation

A semi-discrete periodic approximation of (2) is given by

$$v_{tt} = \tilde{D}_2 v - 3\tilde{D}_2 \bar{v} v - \alpha \tilde{D}_2{}^2 v. \tag{10}$$

Lemma 4. *The discretisation of (2) given by (10) has a local linearisation which is well-posed, as long as the linearisation coefficient $\bar{v}$ fulfills $\bar{v}_{jj} \leq \frac{1}{3} \forall j \in \{0, ..., m-1\}$.*

Proof. Multiplying by v_t^T and adding the conjugate transpose gives

$$\begin{aligned} v_t^T v_{tt} + v_{tt}^T v_t = v_t^T \tilde{D}_2 v + v^T \tilde{D}_2 v_t - 3 v_t^T \tilde{D}_2 \bar{v} v - 3 v^T \bar{v} \tilde{D}_2 v_t \\ - \alpha v_t^T \tilde{D}_2{}^2 v - \alpha v^T \tilde{D}_2{}^2 v_t. \end{aligned}$$

Recognising that $\frac{d}{dt}\left(v^T X v\right) = v_t^T X v + v^T X v_t$ for a symmetric constant matrix X, and approximating $\bar{v}$ as constant, we can rewrite the equation as

$$\begin{aligned} \frac{d}{dt}\|v_t\|_h^2 &= \frac{d}{dt}\left(h v^T \tilde{D}_2 v\right) - 3\frac{d}{dt}\left(h v^T \tilde{D}_2 \bar{v} v\right) - \alpha \frac{d}{dt}\left(h v^T \tilde{D}_2{}^2 v\right) \\ &= \frac{d}{dt}(h v^T (I - 3\bar{v}) \tilde{D}_2 v) - \alpha \frac{d}{dt}(h v^T \tilde{D}_2{}^2 v). \end{aligned}$$

Let us therefore define as the energy of the system

$$\begin{aligned} E &= \|v_t\|_h^2 - (h v^T (I - 3\bar{v}) \tilde{D}_2 v) + \alpha (h v^T \tilde{D}_2{}^2 v), \text{ s.t.} \\ \frac{d}{dt} E &= \frac{d}{dt}\|v_t\|_h^2 - \frac{d}{dt}(h v^T (I - 3\bar{v}) \tilde{D}_2 v) + \alpha \frac{d}{dt}(h v^T \tilde{D}_2{}^2 v) = 0. \end{aligned}$$

As the energy does not grow, we can conclude that the ODE is well-posed. Note that the defined energy exactly mimics the energy in the continous model (6). This also means that, like the continous energy, it is only valid for sufficiently small solutions; we require $(I - 3\bar{v}) \leq 0$ in order for the energy to be valid. It is also possible to estimate the growth in terms of the norm of the solution. Integrating in time gives

$$\|v_t\|_h^2 = \left(h v^T (I - 3\bar{v}) \tilde{D}_2 v\right) - \alpha \left(h v^T \tilde{D}_2{}^2 v\right).$$

As $\tilde{D}_2 \leq 0$, we can conclude that $1 - 3v_j$ should be positive for each j in order to guarantee that the solution does not grow. This means the growth is only bounded for sufficiently small solution magnitudes, just as for the continous model.

□

3.2 Boundary value problem

In this section, the Korteweg-de Vries equation with boundary conditions (4) will be handled using an SBP-SAT spatial discretisation. The boundary conditions are discretised to

$$\begin{aligned} v_0 &= g_1(t) \\ v_m &= g_2(t) \\ d_m v &= h_1(t), \end{aligned} \tag{11}$$

where d_m is the m:th row of the derivation matrix, and $d_m v$ thus approximates u_x at $x = r$. The SBP-SAT discretisation of (4) is given by

$$v_t = -2\bar{v}D_1 v - 2D_1\bar{v}v - D_3 v + SAT, \tag{12}$$

where

$$\begin{aligned} SAT = {} & H^{-1}\left(\tau_1 e_m v_m + \gamma_1 D_1^T d_m^T\right)(v_m - g_1) \\ & + H^{-1}\left(\tau_2 e_0 v_0 + \gamma_2 D_1^T d_0^T\right)(v_0 - g_2) \\ & + H^{-1}\sigma d_m^T (d_m v - h_1). \end{aligned} \tag{13}$$

The SBP matrices D_1 and $D_3 = D_1 D_1 D_1$ are used to approximate the derivatives and an SAT term is added to (weakly) enforce the boundary conditions (11). The SBP operator D_1 can be written as $D_1 = H^{-1}(Q + R)$, where H is a positive diagonal matrix, Q is skew symmetric and

$$R = -\frac{1}{2}e_0^T e_0 + \frac{1}{2}e_m^T e_m.$$

We have also used the element extraction operator e_j, which is a row vector and contains only zeros, except the j:th element which is a one. Note that both boundary points are included as the model is no longer periodic, so the discretisation grid now has $m + 1$ points. It can be shown (see appendix A) that D_3 can also be written on this form, with a somewhat different R term, as

$$D_3 = -H^{-1}\left(D_1^T Q D_1 + D_1^T R D_1 - 2R D_1 D_1\right).$$

Lemma 5. *There exists a set of parameter values for which (12) is a well-posed semi-discretisation of (4) with homogenous boundary data.*

Proof. To ensure well-posedness, we want the SAT term to cancel out any positive terms in the growth of the numeric solution. Thus, the SAT term

must fullfill two conditions: v should converge toward the boundary conditions at the boundary, but it should not grow. By calculating the growth in the other terms, we can determine which terms must be in SAT to fullfill the second condition. Let us define the energy of the system, similarly to the continous model (3), as

$$E = \|v\|_H^2, \tag{14}$$

using the H-norm $\|v\|_H^2 = v^T H v$. Multiplying equation (12) by $v^T H$ and adding the transpose, we have

$$\begin{aligned} E_t &= v_t^T H v + v^T H v_t \\ &= -2v^T H \bar{v} D_1 v - 2v^T D_1^T \bar{v} H v \\ &- 2v^T H D_1 \bar{v} v - 2v^T \bar{v} D_1 H v \\ &- v^T H D_3 v - v^T D_3^T H v \\ &+ v^T H S A T + S A T^T H v. \end{aligned}$$

Now,

$$\begin{aligned} -2v^T H \bar{v} D_1 v - 2v^T D_1^T \bar{v} H v - 2v^T H D_1 \bar{v} v - 2v^T \bar{v} D_1 H v = \\ -2v^T \bar{v}(Q+R)v - 2v^T (Q+R)^T \bar{v} v - 2v^T (Q+R)\bar{v} v - 2v^T \bar{v}(Q+R)^T v \\ = -4v^T \bar{v} R v - 4v^T R \bar{v} v = -8v^T \bar{v} R v = 4(v_0^3 - v_m^3). \end{aligned}$$

Denoting the j:th row of D_1 as d_j, we have

$$\begin{aligned} -v^T H D_3 v - v^T D_3^T H v = 2v^T D_1^T R D_1 v \\ - 2v^T R D_1 D_1 v - 2v^T D_1^T D_1^T R v, \end{aligned}$$

where

$$\begin{aligned} 2v^T D_1^T R D_1 v &= 2(D_1 v)^T R D_1 v \\ &= (D_1 v)^T [-d_0 v, 0..., d_m v]^T \\ &= (d_m v)^2 - (d_0 v)^2, \end{aligned}$$

and

$$\begin{aligned} -2v^T R D_1 D_1 v - 2v^T D_1^T D_1^T R v &= -4v^T D_1^T D_1^T R v \\ &= -4(D_1 v)^T (D_1^T R) v \\ &= [2d_0(D_1 v), 0..., -2d_m(D_1 v)] v \\ &= 2v_0 d_0 D_1 v - 2v_m d_m D_1 v. \end{aligned}$$

Thus, in total,

$$E_t = 4(v_0^3 - v_m^3) - (d_0 v)^2 + (d_m v)^2 - 2v_m d_m D_1 v + 2v_0 d_0 D_1 v + v^T HSAT + SAT^T Hv,$$

and it can be seen that by choosing the parameter values

$$\begin{aligned} \tau_1 &= 2 \\ \tau_2 &= -2 \\ \sigma &\leq -\frac{1}{2} \\ \gamma_1 = 1,\ \gamma_2 &= -1, \end{aligned} \tag{15}$$

the growth induced by the SAT term (13) (excluding boundary data) exactly cancels the growth induced by the differential operators:

$$\begin{aligned} v^T HSAT + SAT^T Hv &= 2v^T \left(2e_m v_m + D_1^T d_m^T\right)(v_m - 0) \\ &\quad + 2v^T \left(-2e_0 v_0 - D_1^T d_0^T\right)(v_0 - 0) \\ &\quad + 2v^T(-\frac{1}{2} d_m^T)(d_m v - 0), \\ &= 4v_m^3 + 2v_m d_m D_1 v \\ &\quad - 4v_0^3 - 2v_0 d_0 D_1 v \\ &\quad - (d_m v)^2 \end{aligned}$$

The resulting energy growth is then

$$E_t = -(d_0 v)^2 \leq 0.$$

Thus, we have a well-posed semi-discretisation which also enforces the desired boundary conditions.

□

4 Computations

4.1 Periodic case

4.1.1 Korteweg-de Vries equation

The semi-discrete Korteweg-de Vries equation (8) is integrated in time using the fourth order Runge-Kutta scheme (sixth and second order derivation operators are used for the spatial discretisation). The analytical soliton solution

num points	error	convergence
33	1.125e-01	
65	5.494e-03	4.5
129	1.234e-04	5.5
257	2.278e-06	5.8
513	3.736e-08	5.9

Table 1: Spatial convergence; periodic model for KdV with 6th order operators. Single wave with wave number $\frac{1}{\sqrt{2}}$, up to time $t = 1$. Discretisation: $k = 0.15h^2$, where $h = L/m$ and $L = 40$.

$u(x,t) = 2k^2 sech^2(k(x - vt - x_0))$ is used to generate the initial condition, with a wave number $k = \frac{1}{\sqrt{2}}$ and wave speed $v = 4k^2$. Using an interval $x \in [-20, 20]$, the function is nearly periodic. A sample solution is shown in Figure (1), where the analytical and numerical solutions are nearly indistinguishable. A sample with a linear combination of three waves of different magnitude interacting with each other is shown in Figure (2). Note how the numerical solution to the triple wave ineraction is not simply the linear combination of the analytical solutions for the respective waves; the wave tops have been displaced after the interaction. A convergence study is also made with respect to the space step h, showing almost sixth order convergence (see Table 1) and second order convergence (see Table2) respectively. This is reasonable considering the operators used. Note that in all tables in this report,

$$\text{error } e \text{ denotes } e = \sqrt{h} \cdot \|u - v\| \tag{16}$$

and

$$\text{convergence denotes } \frac{\Delta \log e}{\Delta \log h}. \tag{17}$$

4.1.2 Boussinesq equation

The semi-discrete Boussinesq equation is also handled with the Runge-Kutta time scheme, after first being rewritten to a first order ODE in time using $x_1 = v$ and $x_2 = v_t$ as

$$\begin{bmatrix} x_1 \\ x_2 \end{bmatrix}_t = \begin{bmatrix} x_2 \\ \tilde{D_2} x_1 - 3\tilde{D_2}\bar{x_1}x_1 - \alpha \tilde{D_2}^2 x_1 \end{bmatrix}.$$

num points	error	convergence
33	3.607e-01	
65	8.486e-02	2.1
129	2.040e-02	2.1
257	5.074e-03	2.0
513	1.271e-03	2.0

Table 2: Spatial convergence; periodic model for KdV with 2nd order operators. Single wave with wave number $\frac{1}{\sqrt{2}}$, up to time $t = 1$. Discretisation: $k = 0.15h^2$, where $h = L/m$ and $L = 40$.

num points	error	convergence
33	1.707e-03	
65	2.836e-04	2.6
129	6.758e-06	5.5
257	1.211e-07	5.8
513	1.971e-09	6.0

Table 3: Spatial convergence; periodic model for Boussinesq with 6th order operators. Single wave with wave number 0.3, up to time $t = 1$. Discretisation: $k = 0.023h^2$, where $h = L/m$ and $L = 80$.

num points	error	convergence
33	4.820e-03	
65	2.686e-03	0.86
129	7.570e-04	1.8
257	1.934e-04	2.0
513	4.869e-05	2.0

Table 4: Spatial convergence; periodic model for Boussinesq with 2nd order operators. Single wave with wave number 0.3, up to time $t = 1$. Discretisation: $k = 0.15h^3$, where $h = L/m$ and $L = 80$.

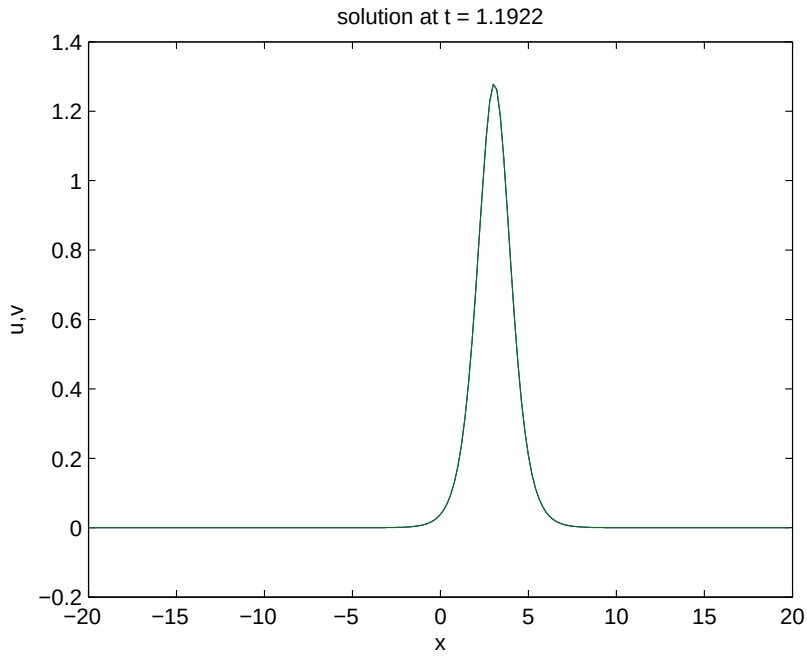

Figure 1: Sample solution to KdV equation (single wave with wave number 0.8) computed with 200 grid points and 6:th order operators

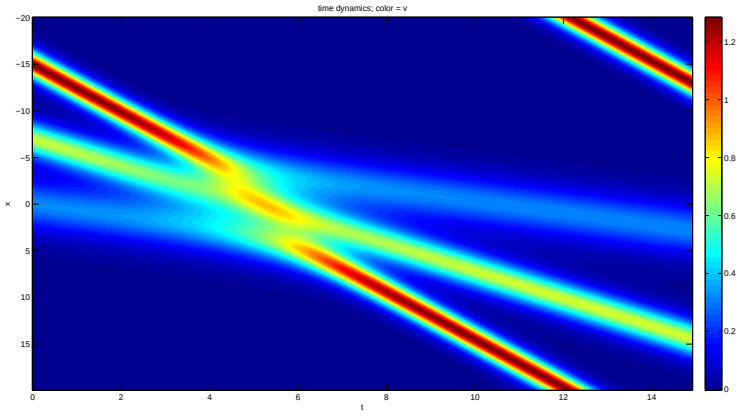

Figure 2: Sample dynamics of KdV equation, three waves with wave numbers 0.8, 0.6 and 0.4, computed on a 400 point grid with 6th order operators.

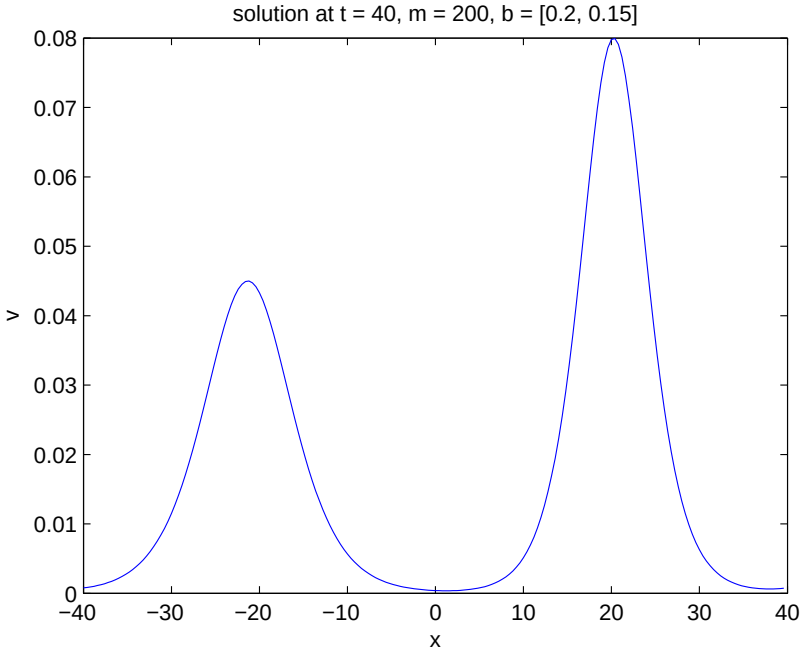

Figure 3: Sample solution to Boussinesq eq.

Using the CFL condition $k < \frac{1}{max(|eig(\tilde{D_2}^2)|)}$ which is an approximation for RK4 based on the principal term, numerical approximations of the solution can be computed and compared to the analytical solution

$$u(x,t) = 2b^2 sech^2(b(x - ct - x0)), \text{ where}$$
$$c = \pm\sqrt{1 - 4b^2}$$

Here the model parameter α is taken to be $\alpha = 1$. With the single soliton test problem, the order of convergence (17) is as expected for the operators; 6.0 for the sixth order operator, see Table (3) and 2.0 for the second order operator, see Table (4). A sample solution for the two wave interaction problem and the corresponding time dynamics are shonw in figures (3) and (4) respectively. In these samples, the initial condition is the sum of two solutions with opposite wave speeds, so the time dynamics shows the collision of the two waves. An interesting observation from Figure (3) is that after the collision, both waves have been displaced backwards in their respective travel directions.

Another interesting feature of the model is that the analytical solution produces purely imaginary wave speeds for any wave number $b > 0.5$. At-

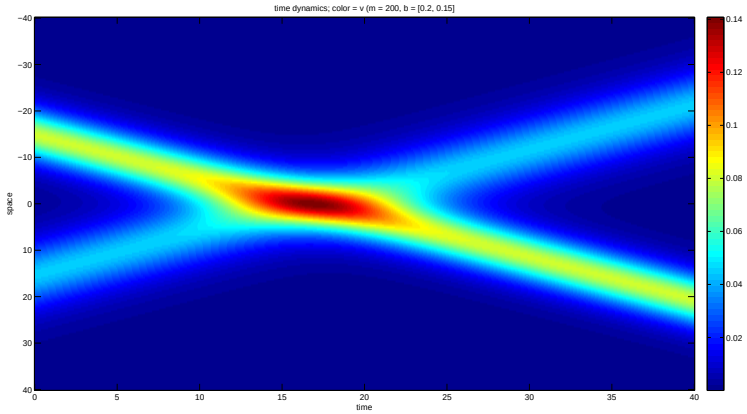

Figure 4: Sample dynamics to Boussinesq eq., waves with $b = 0.2$ and $b = 0.15$, computed on a 200 point grid

tempting to numerically produce these solutions causes the approximation to "blow up", that is it produces a spike that grows in magnitude without bound. Interestingly, this is also the case for any collision of waves where the sum of their wave numbers is greater than 0.5, which is shown by testing collisions with different pairs of wave numbers, and presuming that if the solution blows up for a given pair of wave numbers, it will also blow up if one of the wave numbers is increased. Figure (5) shows, for a sequence of wave numbers b_1, the lowest wave number of the other wave b_2 at which blowup occurs. Though only ten values are tested in each dimension, the result seems to support the hypothesis that blowup occurs wneh $b_1 + b_2 > 0.5$. A similar result was found by Tzirtzilakis et. al. [1].

4.2 Boundary value problem

4.2.1 Estimating accuracy

To estimate the overall order of accuracy of the SBP-SAT discretisation (12), consider as example a D_1 operator of interior order $2p$. With the diagonal norm operator type used in this investigation, the order of accuracy of the operator at the boundary is then p [3]. According to Svärd and Nordström [4], the third derivative matrix operator $D_3 = D_1 D_1 D_1$ will loose one order of accuracy at the boundary per multiplication, so the order of accuracy on the boundaries will be only $p - 2$. However, the principal term in the model is 3rd order, whereby we can expect to reduce the loss of order of accuracy which is due to the boundary interaction by three orders, for the solution in

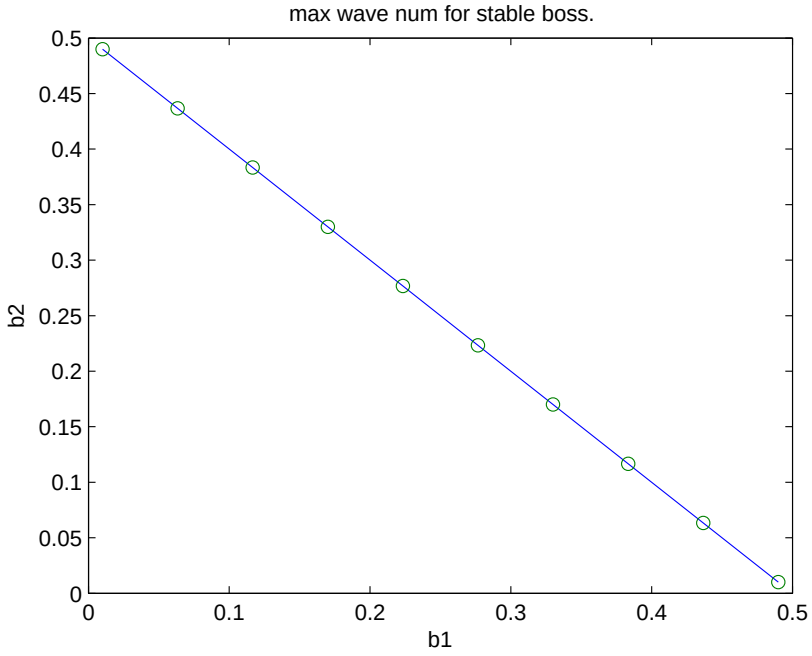

Figure 5: Blowup bounds for pairs of waves

whole. This gives a total order of accuracy of $min(2p, p+1) = p+1 \ \forall p \in \mathbb{N}$. Note that this only applies if the discretisation is stable in an energy sense.

4.2.2 Estimating CFL condition

Writing the model (12) in the form

$$\begin{aligned} v_t &= Mv, \\ M &= -D_1^3 + H^{-1}((D_1^T d_m^T)e_m^T - (D_1^T d_0^T)e_0^T - d_m^T d_m) \end{aligned}$$

where M takes into account only the principal term D_3 and the SAT terms which cancel the energy terms of this operator, we can approximate a CFL condition for the scheme as

$$k < \frac{1}{|\lambda|},$$

for all eigenvalues λ of M (let us take a safe choice of $k = \frac{1}{4max|\lambda|}$).

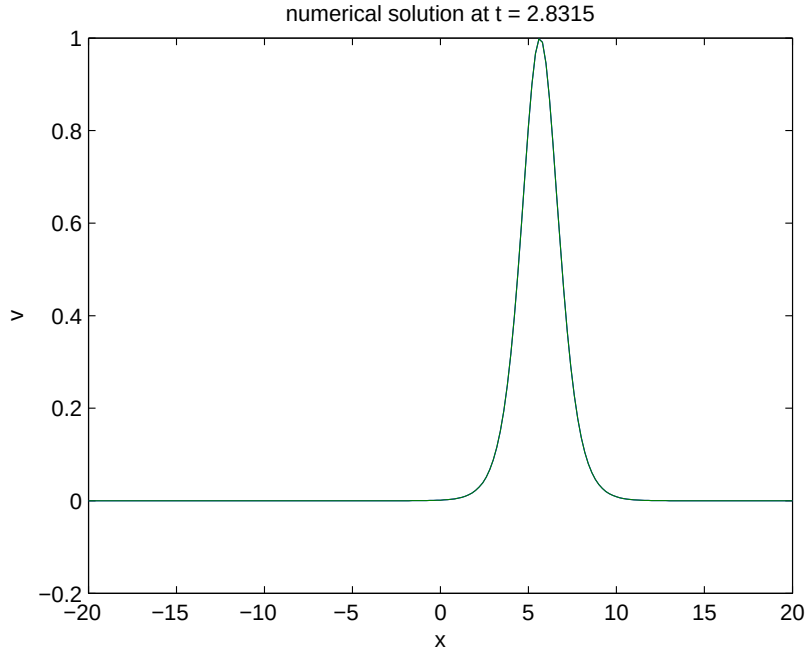

Figure 6: Sample numerical (SBP, $m = 200$) and analytical solution to KdV equation

4.2.3 Test problem

The test problem for the convergence study concists of a soliton with wave number $\frac{1}{\sqrt{2}}$ starting at $x = 10$ and passing through the boundary until time $t = 5$, at wich it is half way through the boundary. Initial and boundary conditions are set to match the analytical solution for this soliton. This test problem is suitable because it contains boundary interactions, but still allows comparing to an analytical reference.

Sample solutions and dynamics are shown in figures (6, 7, 8). The fourth order Runge-Kutta integrator is used when performing a convergence study for the discretisation, the results of which are shown in Tables 5 through 8. Table 9 shows order of convergence of the method per operator, together with the expected outcome.

4.2.4 Standing waves

Another interesting feature of the Korteveg-de Vries boundary value model is that it generates some kind of standing waves. This is illustrated by setting an initial white noise state; the time dynamics in Figure 9 show how this

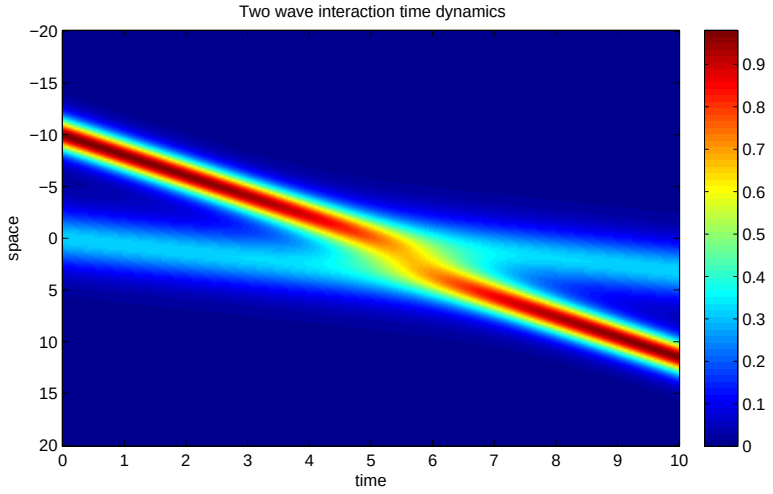

Figure 7: Sample dynamics (SBP, $m = 200$) of KdV equation, 2 waves: one with wave number 0.7 starting at $x = -10$ and one with wave number 0.4 starting at $x = 0$, run to time $t = 10$.

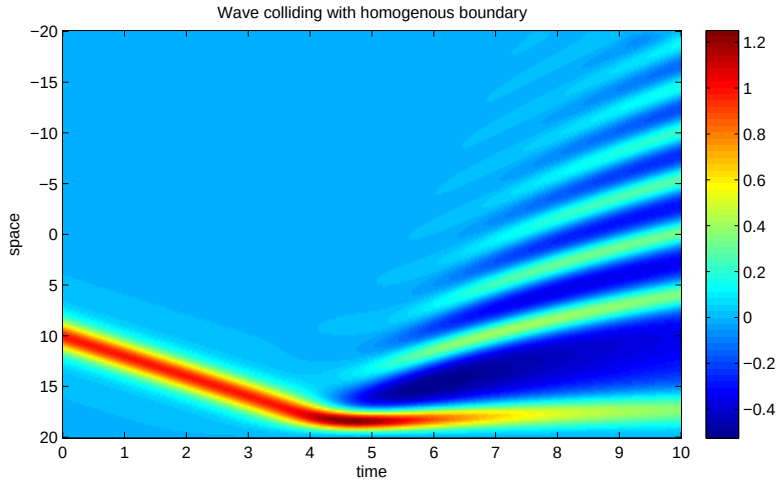

Figure 8: Sample dynamics (SBP, $m = 200$) of KdV equation, wave with wave number 0.7 starting at $x = 10$, run to time $t = 10$: interacting with homogenous boundary.

m	error	convergence
32	6.710e-01	
64	2.644e-01	1.3
128	6.548e-02	2.0
256	1.444e-02	2.2
512	3.530e-03	2.0

Table 5: Spatial convergence (SBP model) for KdV with 2nd order operators. Single wave starting at $x = 10$ with wave number $\frac{1}{\sqrt{2}}$, up to time $t = 5$. Discretisation: $k = 0.24h^3$, where $h = L/m$ and $L = 40$.

m	error	convergence
32	4.414e-01	
64	1.217e-01	1.9
128	9.344e-03	3.7
256	8.728e-04	3.4
512	9.739e-05	3.2

Table 6: Spatial convergence (SBP model) for KdV with 4th order operators. Single wave starting at $x = 10$ with wave number $\frac{1}{\sqrt{2}}$, up to time $t = 5$. Discretisation: $k = 0.12h^3$, where $h = L/m$ and $L = 40$.

m	error	convergence
32	4.502e-01	
64	6.587e-02	2.8
128	1.226e-02	2.4
256	8.650e-04	3.8
512	3.887e-05	4.5

Table 7: Spatial convergence (SBP model) for KdV with 6th order operators. Single wave starting at $x = 10$ with wave number $\frac{1}{\sqrt{2}}$, up to time $t = 5$. Discretisation: $k = 0.063h^3$, where $h = L/m$ and $L = 40$.

m	error	convergence
32	3.610e-01	
64	5.273e-02	2.8
128	3.243e-04	7.3
256	1.280e-06	8.0
512	4.734e-09	8.1

Table 8: Spatial convergence (SBP model) for KdV with 8th order operators. Single wave starting at $x = 10$ with wave number $\frac{1}{\sqrt{2}}$, up to time $t = 5$. Discretisation: $k = 0.0031h^3$, where $h = L/m$ and $L = 40$.

operator ord.	measured conv.	expected conv.
2	2.0	2
4	3.2	3
6	4.5	4
8	8.1	5

Table 9: Spatial convergence (SBP model) per operator

state converges to a standing wave. The boundary conditions in this case are homogenous.

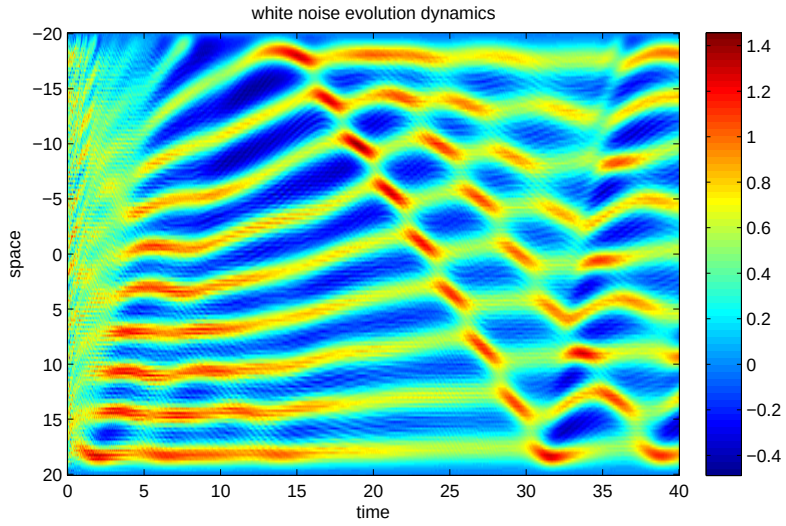

Figure 9: Sample dynamics (SBP, $m = 200$) of KdV equation, initial white noise, run to time $t = 40$: standing wave generated under homogenous boundary conditions.

5 Conclusions and discussion

The Korteweg-de Vries problem is proven to be well-posed, both in the continous model, in the periodic discretisation and in the bounded discretisation. For the Boussinesq equation, well-posedness can only be shown for sufficiently small solution magnitudes, and only under a linearisation. This means that we can only expect a well-posed behaviour for sufficiently small and smooth solutions, and a formal proof of global well-posedness has not been obtained.

Both the periodic and the SBP-SAT finite difference methods show stability and high order of accuracy for the relevant test problems. In the periodic case, convergence matches expectations. For the SBP-SAT scheme, especially the higher order operators are found to give even better convergence than what could be expected. This means the method can be used to simulate solutions accurately within reasonable time. Both schemes also appear to maintain stability even when applied to a wave interaction problem, though this lacks an analytical solution and thus has not been tested. Note that stability was only proven given homogenous boundary data. The initial and boundary value test problem which the SBP-SAT scheme was applied to contains non-homogenous boundary conditions, but the scheme still appeared to evolve in a stable manner.

As observed in the Boussinesq two wave interaction study, the problem is stable approximately as long as the two wave numbers b_1 and b_2 fullfill $b_1 + b_2 < 0.5$. Note that the study was performed for several different levels of grid refinement, all giving the same result. This would indicate that it is indeed a stability region for the PDE, rather than for the discretisation, which is also in agreement with the findings in Tzirtzilakis et. al. [1]. Note that this must be considered as a limitation in the PDE model, with respect to the physical system. It may indicate that a physical system under similar circumstances would produce some turbulent behaviour. We can not expect it to follow the model in these cases as the physical premises for the model can not hold in the state the model is producing (e.g. infintely growing water depth).

A Proof that D_3 is an SBP operator

Given

$$D_1 = H^{-1}(Q + R),$$

where $H > 0$ is diagonal (thus, $H^{-1} > 0$ exists and is diagonal as well), $Q = -Q^T$ and R is zeros except the upper left element which is $-\frac{1}{2}$ and the bottom right element which is $\frac{1}{2}$, all square matrices of the same dimension, we want to show that

$$D_1 D_1 D_1 = -H^{-1}\left(D_1^T Q D_1 + D_1^T R D_1 - 2R D_1 D_1\right). \tag{18}$$

Now,

$$\begin{aligned} D_1^T Q D_1 + D_1^T R D_1 &= D_1^T (Q + R) D_1 \\ &= D_1^T H H^{-1} (Q + R) D_1 \\ &= D_1^T H D_1 D_1, \end{aligned}$$

so

$$\begin{aligned} D_1 D_1 D_1 &= -H^{-1}\left(D_1^T H D_1 D_1 - 2R D_1 D_1\right) \\ &= -H^{-1}\left(D_1^T H - 2R\right) D_1 D_1. \end{aligned}$$

Multiplying by H from the left, we get

$$\begin{aligned} (Q + R) D_1 D_1 &= (-D_1^T H + 2R) D_1 D_1 \\ &= (-\left(H^{-1}(Q + R)\right)^T H + 2R) D_1 D_1 \\ &= (-Q^T H^{-1} H - R H^{-1} H + 2R) D_1 D_1 \\ &= (Q + R) D_1 D_1. \end{aligned}$$

Since the LHS equals the RHS, this proves that equation (18) is true under the given conditions.

References

[1] Ch. Skokos E.E. Tzirtzilakis and T.C. Bountis. Icnaam. In *A numerical study of soliton solutions of the Boussinesq equation using spectral methods*, 2004.

[2] B. Gustafsson, H.-O. Kreiss, and J. Oliger. *Time dependent problems and difference methods*. John Wiley & Sons, Inc., 1995.

[3] Ken Mattsson. Summation by parts operators for finite difference approximations of second-derivatives with variable coefficients. *Journal of Scientific Computing*, 51:650–682, 2012.

[4] M. Svärd and J. Nordström. On the order of accuracy for difference approximations of initial-boundary value problems. *J. Comput. Physics*, 218:333–352, October 2006.